



## Characteristics of lithium-ion batteries during fire tests



Fredrik Larsson <sup>a, b, \*</sup>, Petra Andersson <sup>a</sup>, Per Blomqvist <sup>a</sup>, Anders Lorén <sup>a</sup>, Bengt-Erik Mellander <sup>b</sup>

<sup>a</sup> SP Technical Research Institute of Sweden, Brinellgatan 4, SE-501 15 Borås, Sweden

<sup>b</sup> Department of Applied Physics, Chalmers University of Technology, SE-412 96 Göteborg, Sweden

### HIGHLIGHTS

- Fire tests on commercial lithium–iron phosphate cells and laptop battery packs.
- Heat release rate (HRR) measured, higher state of charge (SOC) gives higher HRR peaks.
- Toxic emissions of HF and  $\text{POF}_3$  (not detected) quantitatively measured.
- Higher total HF emission for lower SOC values.

### ARTICLE INFO

#### Article history:

Received 24 June 2014

Received in revised form

5 August 2014

Accepted 8 August 2014

Available online 15 August 2014

#### Keywords:

Lithium ion

Battery

Hydrogen fluoride

Phosphorous oxyfluoride

Heat release rate

Fire

### ABSTRACT

Commercial lithium-ion battery cells are exposed to a controlled propane fire in order to evaluate heat release rate (HRR), emission of toxic gases as well as cell temperature and voltage under this type of abuse. The study includes six abuse tests on cells having lithium–iron phosphate (LFP) cathodes and, as a comparison, one test on conventional laptop battery packs with cobalt based cathode. The influence of different state of charge (SOC) is investigated and a limited study of the effect of water mist application is also performed. The total heat release (THR) per battery energy capacity are determined to be 28–75 kJ Wh<sup>−1</sup> and the maximum HRR values to 110–490 W Wh<sup>−1</sup>. Hydrogen fluoride (HF) is found in the released gases for all tests but no traceable amounts of phosphorous oxyfluoride ( $\text{POF}_3$ ) or phosphorus pentafluoride ( $\text{PF}_5$ ) are detected. An extrapolation of expected HF emissions for a typical automotive 10 kWh battery pack exposed to fire gives a release of 400–1200 g HF. If released in a confined environment such emissions of HF may result in unacceptable exposure levels.

© 2014 Elsevier B.V. All rights reserved.

### 1. Introduction

Lithium-ion batteries are widely used since they offer great benefits compared to many other battery technologies. Advantages such as high energy and power density, long life time and the possibility of fast charging make them attractive for consumer products and electrified vehicles. Nevertheless Li-ion batteries contain reactive and flammable materials, therefore safety issues are a concern and a number of incidents involving Li-ion batteries have been reported over the last couple of years [1–4]. Overheating of the batteries may result in exothermal reactions and lead to a thermal runaway with excessive amounts of heat, gas emissions,

fire and potentially explosion/rapid disassembling [1,5–6]. Even in case there is no thermal runaway, a heated battery can still vent flammable and toxic gases. Examples of toxic gases that may originate from such events are hydrogen fluoride, HF, and phosphorous oxyfluoride,  $\text{POF}_3$ . The toxicity of HF is quite well known [7] since it is formed during several chemical decomposition processes and fires but the toxicity of the  $\text{POF}_3$  is currently unknown. Actually, the toxicity of  $\text{POF}_3$  might act with other poisoning mechanisms than just by formation of three equivalents of HF. Therefore, critical limits of exposure might be lower for  $\text{POF}_3$  than for HF as in the chlorine analog  $\text{POCl}_3/\text{HCl}$  [8]. The origin of the fluorine compounds is primarily the battery electrolyte but emissions can also come from the binder (e.g. PVdF) of the active electrode materials. The electrolyte usually contains flammable organic solvents some of which are volatile at modest temperatures (below 100 °C) and the commonly used Li-salt, lithium hexafluorophosphate,  $\text{LiPF}_6$ , has a limited thermal stability upon

\* Corresponding author. Department of Applied Physics, Chalmers University of Technology, SE-412 96 Göteborg, Sweden. Tel.: +46 10 5165928; fax: +46 33 125038.

E-mail addresses: [fredrik.larsson@sp.se](mailto:fredrik.larsson@sp.se), [vegan@chalmers.se](mailto:vegan@chalmers.se) (F. Larsson).

heating. The decomposition of  $\text{LiPF}_6$  can be described, according to Yang et al. [9] and Kawamura et al. [10], by:



When  $\text{LiPF}_6$  is heated in a dry and inert atmosphere it decomposes to lithium fluoride,  $\text{LiF}$ , which is a solid compound at temperatures below  $845^\circ\text{C}$  and phosphorus pentafluoride,  $\text{PF}_5$ , which is a gas and a strong Lewis acid, see Eq. (1). In the presence of water/moisture  $\text{PF}_5$  produces  $\text{POF}_3$ , and  $\text{HF}$  (Eq. (2)).  $\text{LiPF}_6$  can also react directly with water/moisture to form  $\text{LiF}$ ,  $\text{POF}_3$  and  $\text{HF}$  according to Eq. (3). In fact,  $\text{LiPF}_6$  is highly susceptible to hydrolysis by even trace amounts of moisture [11]. Furthermore, Kawamura et al. [10] suggested that  $\text{POF}_3$  could react with water and form  $\text{POF}_2(\text{OH})$  and  $\text{HF}$  according to Eq. (4).

The decomposition of electrolytes containing  $\text{LiPF}_6$  forming  $\text{HF}$  is complex and has mainly been studied at ambient temperature and during heating (but not in situations where there is a fire) [12–19]. Besides emissions containing fluorine and vaporized solvents, a Li-ion cell can also emit other gases, e.g.  $\text{H}_2$ ,  $\text{CO}$ ,  $\text{CO}_2$ ,  $\text{CH}_4$ ,  $\text{C}_2\text{H}_6$  and  $\text{C}_2\text{H}_4$  [20–22]. Gases can actually be emitted from batteries under several types of abuse conditions such as overheating, overcharge [23], short circuit, fires etc. A few studies are published on heat release rate (HRR) and emissions of toxic gases from Li-ion batteries in fire conditions. Ribière et al. [24] used a Tewarson fire calorimeter to study the HRR and toxic gases from commercial 2.9 Wh pouch cells with  $\text{LiMn}_2\text{O}_4$  (LMO) cathode and graphite anode and found e.g. that the total  $\text{HF}$  release was higher for lower state of charge (SOC) values. Eshetu et al. [25] studied fire properties and toxicity for commonly used Li-ion battery electrolytes but without Li-salt and thus without the possibility to produce  $\text{HF}$ .

This paper presents results from fire tests of commercially available Li-ion battery cells. Parameters such as heat release rate, cell voltage and surface temperature are measured as well as  $\text{HF}$  and  $\text{POF}_3$  emissions. The influence of application of water is examined to a limited extent by introducing water mist into the flames.

## 2. Experimental

The tests were conducted using the measurement and gas collection system of a Single Burning Item (SBI) apparatus, that is normally used for classification of building materials according to the European Classification scheme EN13823 [26]. The experimental setup is shown in Fig. 1. The cells/batteries were placed on a wire grating (large gratings about  $4\text{ cm} \times 10\text{ cm}$ ) as seen in Fig. 2. A propane burner was placed underneath the cells/batteries and was ignited two minutes after the start of the test. The HRR of the burner alone was approximately 15 kW. Abuse tests were performed on 7 Ah EIG LFP pouch cells, 3.2 Ah K2 LFP cylindrical cells, and on 16.8 Ah Lenovo laptop battery packs, see Table 1.

Test 1–5 used commercially available pouch cells with lithium–iron phosphate (LFP),  $\text{LiFePO}_4$ , cathode and carbon based anode. Each test consisted of five cells that were mechanically fastened together with steel wire (0.8 mm diameter). The terminal tabs of the cells were cut for all cells but the mid one (the third cell), for which the cell voltage was measured. On both sides of the third cell type K thermocouples were centrally attached measuring the cell surface temperature. Temperature values presented in this

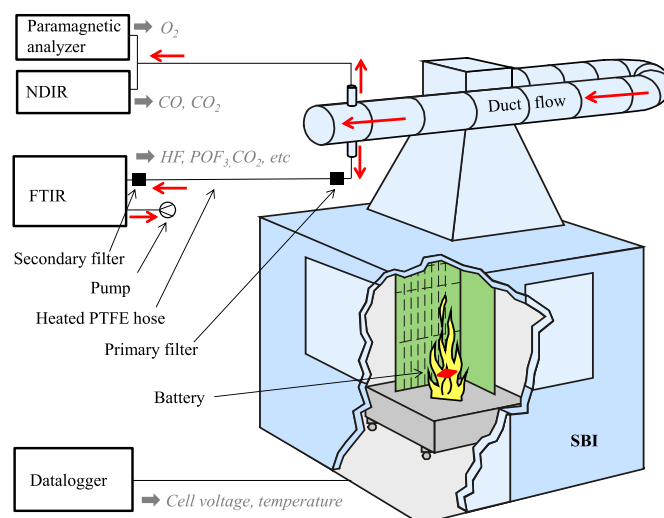


Fig. 1. Schematic illustration over experimental setup.

paper are the average of these thermocouple readings. The temperature and cell voltage was measured with a sample rate of 1 Hz using a data logger, Pico Technology ADC-24. In test 3, water mist was manually applied as a spray into the flames above the battery to study any influence from additional water on the composition of the gas emissions. In test 6, nine K2 26650-cells, i.e. cylindrical cells 26 mm in diameter and 65 mm long, were placed standing up next to each other inside a box. The box had side walls made of non-combustible silica board and steel net at the bottom and top. It was used as a safety precaution to avoid possible projectiles. In test 7, two identical laptop battery packs were used and placed inside a steel net and fastened on the wire grating.

The cells in test 1–6 were set to the selected SOC-level, according to Table 1, by a charge/discharge procedure using an ordinary laboratory power aggregate and a Digatron battery test equipment. The two laptop battery packs in test 7 were fully charged using a laptop computer. All batteries were unused but had different calendar aging. The EIG cells were approximate 2–3 years old, the K2 cells were approximate 1–2 years old and the laptop battery pack was less than 6 months old.

The laptop battery packs in test 7 differ from the other test objects. First, they consist of not only the cells but also electrical connectors, plastic housing and electronic circuits. Secondly, they



Fig. 2. The 5-cells pack of EIG cells placed on a wire grating.

**Table 1**  
Test objects.

Test no.	Battery type	No. of cells	Nominal capacity (Ah)	Weight (g)	Test condition
1	EiG ePLB-F007A	5	35	1227.9	100% SOC
2	EiG ePLB-F007A	5	35	1229.7	100% SOC
3	EiG ePLB-F007A	5	35	1229.3	100% SOC + water mist
4	EiG ePLB-F007A	5	35	1228.6	0% SOC
5	EiG ePLB-F007A	5	35	1227.6	50% SOC
6	K2 LFP26650EV	9	28.8	734.8	100% SOC
7	Lenovo laptop battery packs	12 <sup>a</sup>	33.6	639.0	100% SOC

<sup>a</sup> Two laptop battery packs were used at the same time, each with 6 cells.

have cobalt based cell chemistry with a higher cell voltage, 3.7 V vs 3.2 V for the LFP-cells. Thirdly, in each battery pack, 3 cells are electrically connected in series increasing the voltage to 11.1 V.

All tests were video recorded. The tests were performed during two days and in the beginning of each day a blank test was conducted in order to be able to subtract the burner influence on the HRR values and to make a blank for the gas analysis. The burner was active for a varying duration in the different tests, between 17 and 32 min, i.e. as long as a heat release contribution from the battery was still present. The fire emissions from the test object were collected in a ventilation duct. In test 1–2 a duct flow of  $0.6 \text{ m}^3 \text{ s}^{-1}$  was used but in order to increase emission concentrations in the ventilation the duct flow was decreased to  $0.4 \text{ m}^3 \text{ s}^{-1}$  in test 3–7.

A *Servomex 4100 Gas purity analyser* was used to measure the oxygen content of the flow by a paramagnetic analyzer and CO and CO<sub>2</sub> were determined by a non-dispersive infrared (NDIR) sensor. The HRR was calculated using the method of oxygen consumption and was corrected for CO<sub>2</sub> [26]. A part of the flow in the ventilation duct was extracted for on-line FTIR analysis. This sub-flow was extracted through an 8.5 m sampling PTFE hose, heated to 180 °C, using a pump ( $3.5 \text{ L min}^{-1}$ ) located after the FTIR measurement cell. The sampled gas is passed through a primary filter (*M&C* ceramic filter, heated to 180 °C) before the heated hose and thought a second filter (*M&C* sintered steel filter, heated to 180 °C) before the FTIR. After each test the primary filter was chemically analyzed for fluoride content since it is known that HF may be partly adsorbed by this type of filter [27]. The fluoride adsorbed by the filter was determined by method B.1 (b) of the SS-ISO 19702:2006 Annex B standard, where the filter is leached in water in an ultrasonic bath for at least 10 min. Thereafter the fluoride content in the water is measured by ion chromatography with a conductive detector. The amount of HF is calculated by assuming that all fluoride ions present in the filter derives from HF. The concentration of the emitted gas was measured by Fourier transform infrared spectroscopy (FTIR) using a *Thermo Scientific Antaris IGS analyzer (Nicolet)* with a gas cell. The spectral resolution of the FTIR was  $0.5 \text{ cm}^{-1}$ . The gas cell was of 0.2 L, had a path length of 2.0 m, a cell pressure of 86.7 kPa was maintained and the cell was heated to 180 °C. Each spectrum used 10 scans which gave a new spectrum every 12 s. There is a natural time delay between the gas measurement of the SBI and the FTIR in the measurement setup. The HRR and FTIR results presented in this paper were therefore time synchronized by overlaying of CO<sub>2</sub> measurements from the FTIR and the NDIR.

FTIR is a suitable technique to measure the concentrations of HF and POF<sub>3</sub> in the emitted fire gases. The FTIR was calibrated for a number of compounds, e.g. HF, when delivered from the supplier. However, it was found that the HF calibration was not accurate enough so it was recalibrated, see Andersson et al. [28] for a detailed description of the calibration procedure. The FTIR was also calibrated for POF<sub>3</sub>. PF<sub>5</sub> could only be qualitatively determined by its spectral signature [28] but no traces of PF<sub>5</sub> could be found in the

**Table 2**The spectral bands used for HF and POF<sub>3</sub>.

Spectral bands ( $\text{cm}^{-1}$ )	Type of band
HF	
4203–4202	HF R-branch stretching mode [29]
4175–4172	HF R-branch stretching mode [29]
POF <sub>3</sub>	
1418–1413	P–O stretching mode [9]
874–868	P–F symmetric stretching mode [9]

fire tests probably due to that the PF<sub>5</sub> is highly reactive. The detection limits were 2 ppm for HF and 6 ppm for POF<sub>3</sub>. The spectral bands used for Classical Least Square (CLS) type quantification of HF and POF<sub>3</sub> are stated in Table 2.

### 3. Results and discussion

The HRR results for the EiG battery cells with 0%, 50% and 100% SOC are shown in Fig. 3. High SOC values give high HRR peaks and the temperature and voltage measurements in Fig. 4 confirm that cells with high SOC value give a more reactive response, with rapid temperature increase and earlier voltage breakdown. Studies using other techniques confirm our results that battery cells with higher SOC are more thermally reactive, using e.g.; fire calorimeter [24], accelerating-rate calorimetry (ARC) [5] and VSP2 adiabatic calorimeter [30]. The HRR from the nine K2 cells in test 6 and the two complete laptop battery packs in test 7 can be seen in Fig. 5. The laptop pack includes the plastic box and have Li-ion cells with the more reactive cobalt based cathode, while the K2 cells (as well as the EiG cells) have LFP cathodes which are known to be significantly more stable [5,31–34]. The higher HRR values for the laptop cells are thus expected.

Outbursts from fully charged cells (100% SOC) of EiG, K2 and laptop packs were visually observed, see Fig. 6 for a typical example. The outbursts originate from ignition of the rapid gas release from a cell upon opening due to excessive cell pressure and correspond to the sharp spikes in the HRR curves, see Figs. 3 and 5. In most cases, one HRR-spike could be detected for each individual cell. For EiG cells with 50% and 0% SOC no spikes were observed in the HRR curves, instead two broad maxima were found. The orientation of the cells on the wire grating varied due the different packaging types (pouch, cylindrical, complete battery pack) which might have influenced the results. However, tests 1–5 used the same cell type and setup. The results of tests 6–7 can be seen as examples of possible events for these types of cells.

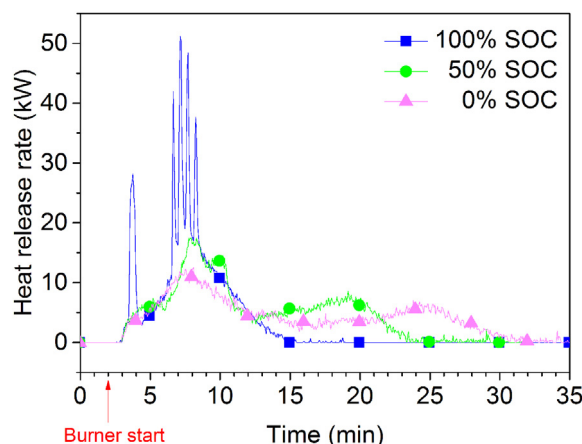


Fig. 3. Heat release rate for EiG cells with 0%, 50% and 100% SOC.

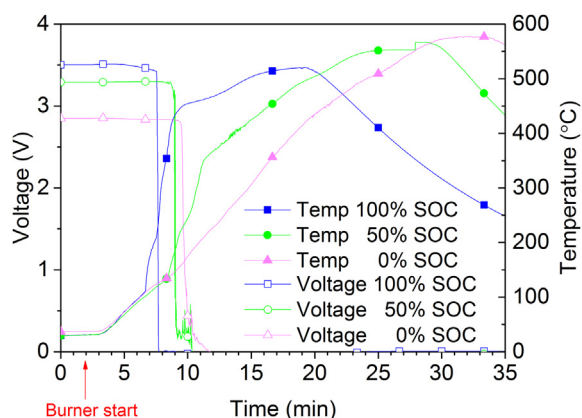


Fig. 4. Mid cell temperature and voltage for EiG with 0%, 50% and 100% SOC.

The fire test on EiG cells with 100% SOC was repeated two times (tests 1–2) without water mist application and one time (test 3) with water mist applied approximately 6.5 min after burner start. Fig. 7 shows HRR, HF emission rate, voltage and temperature for the mid cell, in test 2. Rapidly propagating flames released from the battery cells were visually observed five times during the test and denoted outbursts, marked in Fig. 7, and coincided with the five spikes in the HRR curve. The hydrogen fluoride concentration showed a rapid increase at the end of the HRR peak and the HF maximum plateau was reached just after the HRR spikes. The delay between HF production and HRR is not due to gas transport time since it is compensated by CO<sub>2</sub> synchronization, the reason is due to delay times in the sampling system. As expected, the temperature of the mid cell showed a steep increase connected to the HRR peaks, the outbursts and the voltage breakdown. The maximum temperature reached in this measurement was 521 °C. Test 1 and test 2 show similar values and behavior, the variation between the tests is due to the nature of the fire characteristics.

Fig. 8 shows test 3 where 100% SOC EiG cells were tested with water mist application. Most of the results of the tests with and without water mist are similar, but the maximum HF concentration recorded at the time of applying the water mist into the flames is approximately twice as high as that in tests 1–2. However, the total amount of measured HF from FTIR and absorbed by the primary filter is of the same order for all tests 1–3. The water mist was certainly not the only source of water in this experiment, in addition to water existing in the atmosphere water is produced by the

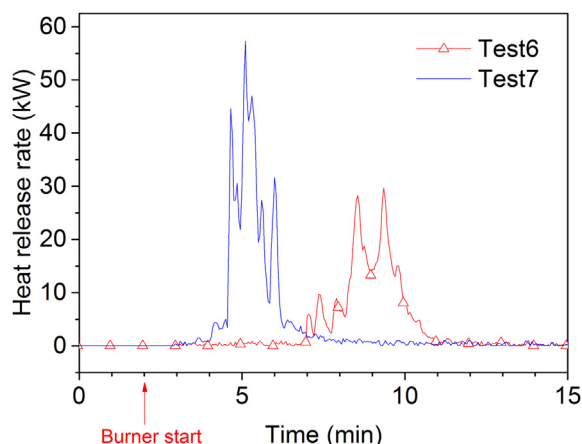
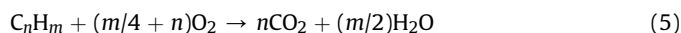


Fig. 5. Heat release rate for K2 cells (test 6) and laptop battery packs (test 7).

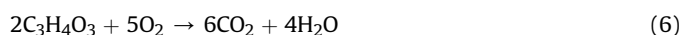


Fig. 6. Outbursts from EiG 100% SOC (test 1).

combustion process. In the general case of combustion of hydrocarbons water is produced:



and in the oxidation of ethylene carbonate (EC), C<sub>3</sub>H<sub>4</sub>O<sub>3</sub>, a commonly used Li-ion solvent, water is thus produced according to:



When propane, C<sub>3</sub>H<sub>8</sub>, is combusted, 1 mol of propane produces 4 mol of water according to Eq. (5). In test 1–3 the 15 kW propane burner was active during 17 min and given the heat of combustion of propane, 2044 kJ mol<sup>−1</sup>, the amount of water produced from the burner can be calculated to be approximately 550 g.

The water concentration in the exhaust duct was measured by the FTIR, see Fig. 9 for the results of test 1–3. The water concentration shown for test 3 is scaled (factor 0.4/0.6) due to the lower duct flow in order to allow a comparison with the measured values of test 1–2. The outbursts result in an increased water concentration and the effects on the measured water concentration from the applied water mist is also clearly seen. Calculated from the measured data, the mass of the added water mist was around 400 g

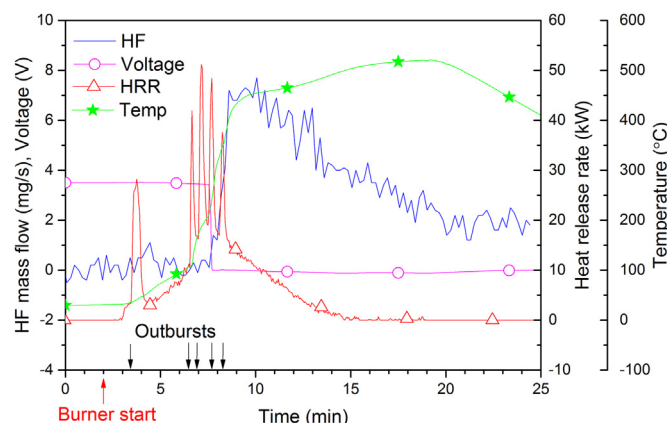


Fig. 7. Resultsf EiG 100% SOC (test 2).

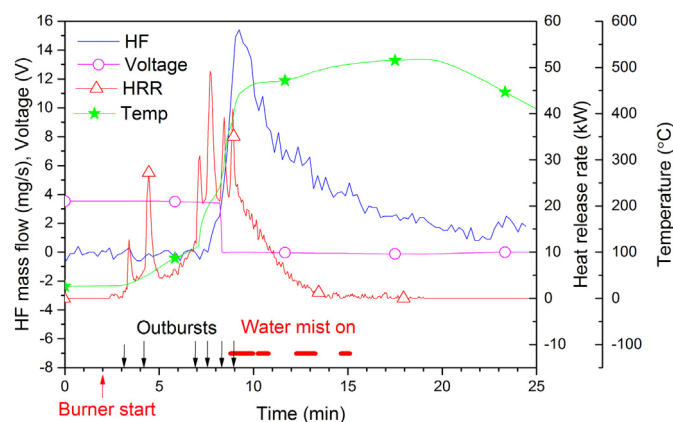


Fig. 8. Results for EiG 100% SOC with water mist (test 3).

while around 350 g water was released due to the combustion of battery materials. The water in the duct flow from ambient air was around 1500 g for test 3 and 2300 g in test 1–2 (due to higher duct flow rate). The time of the water mist application was relatively short and the water mist was applied in the reaction zone, thus the impact from this source of water was potentially high which is also seen in Fig. 9. The amounts of water from ambient air were large but the impact should have been low since only part of the air flow passed the reaction zone above the battery and no effect on the HF concentration was observed due to the higher ambient water content in the duct flow in test 1–2 compared to test 3. Fig. 10 shows the correlation between HF production and water concentration for test 3. No HF production directly associated with the outbursts can be seen but the application of water mist seems to influence the HF production. However, the added water mist only temporarily increased the emission of HF but did not change the total amount of HF produced. Anyhow, only one test with water mist application was performed and the correlation between the water mist application and the increased HF peak production could possibly depend on other factors than the additional water introduced by the water mist.

Fig. 11 shows the measured production rate of HF for all EiG tests. For 0–50% SOC the peaks are broadened compared to the peaks for the 100% SOC cells and the total amount of measured HF is about double that of the 100% SOC cells. Detailed results from all the tests can be found in Table 3. Total yields in  $\text{mg g}^{-1}$  are calculated as total amount of HF divided per weight loss of the batteries.

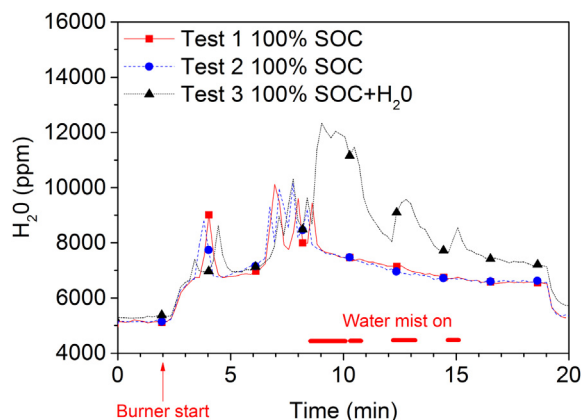


Fig. 9. Water concentrations measured in test 1–3. The increased water level in test 3 due to water mist application is clearly seen.

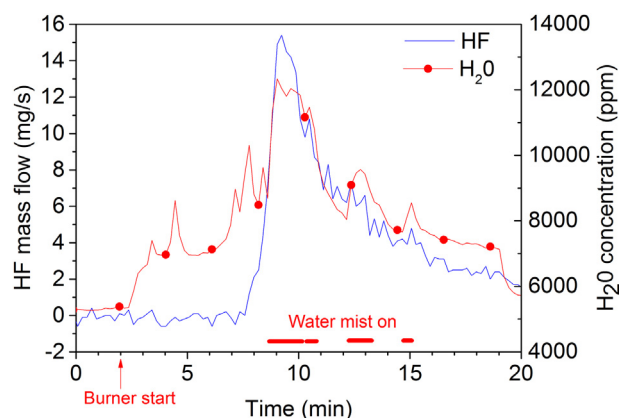


Fig. 10. HF mass flow and water concentration for test 3.

In test 7 the weight loss also included the burning of pack materials, e.g. plastic housing. Total yields in  $\text{mg Wh}^{-1}$  are calculated as total amount HF in mg divided by total energy capacity, Wh, of the batteries for each test. Whichever of these yield values that are used, the EiG cells with 0% or 50% SOC showed the highest HF values. The measured data indicate a relationship between SOC and the total released HF emissions, with increased total amounts of HF emission for lower SOC. Ribière et al. [24] found somewhat similar results by studying single cells with 100%, 50% and 0% SOC, showing an increasing total amount of HF emissions for decreasing SOC value. The reason for this is unknown and an investigation of the relationship would require further studies. The HF concentrations measured were in all cases well above the detection limit but no significant amounts of  $\text{POF}_3$  could be detected in any of the tests. FTIR measurements on samples of similar electrolytes with  $\text{LiPF}_6$  in a cone calorimeter have shown the production of  $\text{POF}_3$  to be in the order of 1/20 of the HF production [28]. The detection limit of  $\text{POF}_3$  in the FTIR measurements is 3 times higher than for HF, thus there could have been  $\text{POF}_3$  present during the measurements which has not been detectable.

The HRR values presented in this paper are calculated using the oxygen consumption method. This technique is well accepted and used in fire calorimetry measurements. For the case of battery fires, the technique might however have some limitations since it will not account for energy liberated by Joule heating through electrical

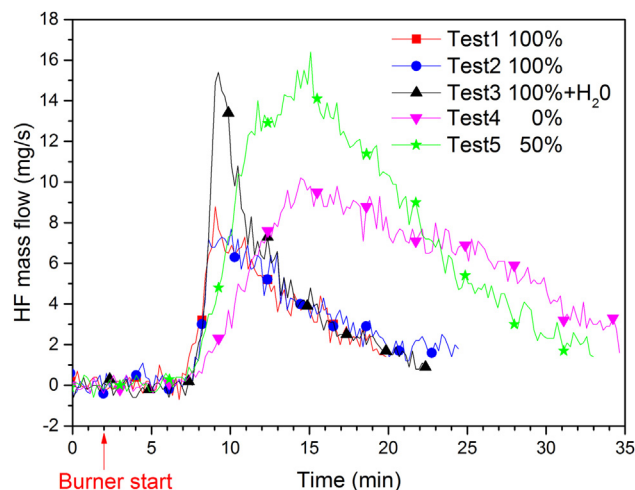


Fig. 11. HF mass flow for EiG cells with different SOC (indicated by % in figure legend) in tests 1–5.

**Table 3**

Detailed results of heat release rate, energy release, hydrogen fluoride emissions for test 1–7.

Test no.	Weight loss (g)	Max heat release (kW)	Total heat release (kJ)	Hydrogen fluoride					
				Max production rate (g s <sup>-1</sup> )	Total amounts from FTIR (g)	Total amounts from filter (g)	Total amounts (g)	Total yields (mg g <sup>-1</sup> )	Total yields (mg Wh <sup>-1</sup> )
1	346	55	7731	0.0088	3.2	1.7	4.9	14	44
2	342	51	7526	0.0077	3.9	2.4	6.3	18	56
3	341	49	8095	0.0154	4.2	1.5	5.7	17	51
4	353	13	8314	0.0102	9.7	1.6	11.3	32	100
5	354	17	8452	0.0164	12.0	1.9	13.9	39	120
6	145	29	2766	0.0029	1.2	1.0	2.2	15	24
7	258	57	3470	0.0011	Not detected	1.9	1.9	7.3	15

discharge, e.g. internal short circuits in a cell due to melted separator. Ribière et al. [24] estimates the error to be max 10% and thereby claim the oxygen consumption method to be usable. Besides the issue with Joule heating, the Li-ion battery can release its own oxygen [5]. The oxygen release varies with different Li-ion cell chemistries, and is typically lowest for LFP. In this test method a large amount of air is passed in the duct flow and the effect of released oxygen is regarded as negligible.

In order to simplify an estimation of the heat and gas emission hazards for this type of lithium-ion batteries the values have been normalized to the energy capacity of the batteries. Table 4 shows such values from our study as well as calculated values using data from Ribière et al. [24]. Again, note that the values for the laptop battery pack also accounts for the plastic housing. The EiG cells have about the double total heat release, 67–75 kJ Wh<sup>-1</sup>, compared to the other batteries in Table 4. Also, the influence of SOC levels is small compared to the differences between the battery types. The maximum HRR per Wh calculated from our experimental data, 110–490 W Wh<sup>-1</sup>, is, however, lower than the values reported by Ribière et al. [24], 300–1900 W Wh<sup>-1</sup>, who used a different test procedure. Normalized values for the total HF release vary in our study between 15 and 124 mg Wh<sup>-1</sup>, a wider range than that found by Ribière et al. [24].

In general, the measured values of the amount of HF produced in fire tests are comparatively high and could pose a serious hazard if released in an enclosed environment. For example, the 7 Ah EiG battery cell can typically be used in a plug-in electric vehicle (PHEV) and a 10 kWh battery pack of a PHEV could consist of 448 such cells (a battery system of 112 cells in series and 4 cells in parallel; cell voltage 3.2 V nominal, pack voltage 358.4 V nominal). If we extrapolate our results for the 5-cell packs by multiplying by a factor of 448/5 = 89.6, it may represent a scenario of a complete fire of a PHEV battery pack. The extrapolation gives 400–1200 g HF depending on the state of charge for the EiG cells where high SOC gives lower HF. Even though the extrapolation is extensive and therefore can be questionable the result is in the same order of magnitude as that reported by Lecocq et al. [35] who conducted

complete vehicle fire tests including HF measurements of two electric vehicles (EV) with fully charged batteries (100% SOC) and on two similar gasoline powered combustion engine passenger cars (none-EV). Lecocq et al. [35] measured significant HF emissions from all four vehicles, both EV and similar none-EV, and suspected that the HF emissions from all vehicles could in part originate from air conditioner system. Using the values in Lecocq et al. [35], and calculating the difference in total HF release between the EV and the similar none-EV an estimate of the contribution to the HF release from the Li-ion battery can be found to be 919 g for a 16.5 kWh Li-ion battery and 657 g for a 23.5 kWh Li-ion battery. Scaling these values for a 10 kWh battery results in 280–557 g of released HF.

If we assume that all the emitted HF is released within a closed passenger compartment of 5 m<sup>3</sup> of an electrified vehicle we obtain HF concentrations between 80 and 240 g m<sup>-3</sup>. NOISH (The National Institute for Occupational Safety and Health) in USA stated the IDLH (Immediately Dangerous To Life or Health) value for HF to 30 ppm corresponding to a concentration of HF in air of 0.025 g m<sup>-3</sup> [7]. Our values which are similar to those of Lecocq et al. [35] exceed the IDLH by about four orders of magnitude. The reported HF values from Ribière et al. [24] also by far exceed the IDLH value. However, the experimental data reported here comes from a limited study and the calculation assumes a somewhat extreme theoretical situation which differs from real fire situations, i.e. all HF is emitted and trapped in the compartment and that the passenger stays in the compartment. Anyhow, even if the emission occurs in a much larger volume, e.g. in a garage, the HF levels can still be very high. The reported HF values thus indicate that a critical situation might occur in the case of a thermal event in a Li-ion battery pack. Although we could not directly detect the presence of POF<sub>3</sub>, it may also be present in considerable amounts since indications are that HF and POF<sub>3</sub> is produced with a ratio of about 1:20 [28].

#### 4. Conclusions

The tests show that lithium-ion battery cells exposed to fire are significantly more reactive at 100% SOC than at lower SOC values and energetic outbursts were observed. The HRR peak values thus varied in a rather wide range, between 13 and 57 kW for batteries with approximately 100 Wh energy capacity. The normalized total heat release per energy capacity was 28–75 kJ Wh<sup>-1</sup> and the normalized maximum HRR values were 110–490 W Wh<sup>-1</sup>.

The amount of HF released varied between 15 and 124 mg Wh<sup>-1</sup>. Lower SOC values gave higher amounts of HF. Extrapolation of data shows that the potential HF release from a 10 kWh PHEV battery is in the range 400–1200 g HF. If this amount of HF would be released inside a passenger compartment of 5 m<sup>3</sup> the HF concentration would be 80–240 g m<sup>-3</sup>, that is magnitudes higher than acceptable short time exposure levels. Besides HF, there may also be significant emissions of POF<sub>3</sub>, a compound which might be more toxic than HF.

**Table 4**

Total heat release, maximum HRR value and total HF release, normalized values for energy capacity.

Battery	Nominal energy capacity (Wh)	Normalized total heat release (kJ Wh <sup>-1</sup> )	Normalized maximum HRR (W Wh <sup>-1</sup> )	Normalized total HF release (mg Wh <sup>-1</sup> )
Five EiG cells	112	67–75	110–490	44–124
Nine K2 cells	92	30	310	24
Two laptop battery packs	124	28	460	15
Single cell, calculated from Ribière et al. [24]	11	28–35	300–1900	37–69

Although these estimates are based on an extrapolation and can be regarded as a hypothetical case it highlights the risks associated with toxic emissions at battery fires and the need to find replacements for the fluorine content in the Li-salt and binder used in Li-ion battery cells. The influence of additional water in form of water mist seemed to increase the HF emissions momentarily, however the total HF release was the same. Further studies of the relationship between water and HF emissions in fires are needed in order to thoroughly evaluate potential risks related to the use of water as firefighting medium in electric vehicle fires.

## Acknowledgments

The authors gratefully acknowledge the Swedish Energy Agency and the FFI-program as well as the Swedish Fire Research Board for financial support. Several persons at SP Fire Technology are acknowledged for their contribution to this work, including Lars Pettersson and Magnus Samuelsson.

## References

- [1] Z.J. Zhang, P. Ramadass, W. Fang, in: G. Pistoia (Ed.), *Lithium-ion Batteries Advances and Applications*, Elsevier, Amsterdam, 2014, pp. 409–435.
- [2] Q. Wang, P. Ping, X. Zhao, G. Chu, J. Sun, C. Chen, *J. Power Sources* 208 (2012) 210–214.
- [3] D. Lisbona, T. Snee, *Process Saf. Environ. Prot.* 89 (2011) 434–442.
- [4] <http://edition.cnn.com/2014/01/14/travel/787-dreamliner/>, 2014-05-13.
- [5] D. Doughty, E.P. Roth, *Electrochem. Soc. Interface* (Summer 2012) 37–44.
- [6] F. Larsson, P. Andersson, B.-E. Mellander, in: B. Sandén, P. Wallgren (Eds.), *Systems Perspectives on Electromobility*, Chalmers University of Technology, Göteborg, 2014, ISBN 978-91-980973-9-9, pp. 33–44.
- [7] Documentation for Immediately Dangerous to Life or Health Concentrations (IDLHs) for Hydrogen Fluoride (as F), The National Institute for Occupational Safety and Health (NIOSH), USA, May 1994. <http://www.cdc.gov/niosh/idlh/7664393.html>.
- [8] Middelmann, *Hygiensiska gränsvärden AFS 2011:18*, Hygieniska gränsvärden Arbetsmiljöverkets föreskrifter och allmänna råd om hygieniska gränsvärden, Swedish Work Environment Authority, Sweden, 2011, ISBN 978-91-7930-559-8. ISSN:1650-3163.
- [9] H. Yang, G.V. Zhuang, P.N. Ross Jr., *J. Power Sources* 161 (2006) 573–579.
- [10] T. Kawamura, S. Okada, J.-i. Yamaki, *J. Power Sources* 156 (2006) 547–554.
- [11] Q.-S. Wang, J.-H. Sun, G.-Q. Chu, X.-L. Yao, C.H. Chen, *J. Therm. Anal. Calorim.* 89 (1) (2007) 245–250.
- [12] C.G. Barlow, *Electrochem. Solid-State Lett.* 2 (8) (1999) 362–364.
- [13] S.E. Sloop, J.B. Kerr, K. Kinoshita, *J. Power Sources* 119–121 (2003) 330–337.
- [14] C.L. Campion, W. Li, W.B. Euler, B.L. Lucht, B. Ravdel, J.F. DiCarlo, R. Gitzendanner, K.M. Abraham, *Electrochem. Solid-State Lett.* 7 (7) (2004) A194–A197.
- [15] C.L. Campion, W. Li, B.L. Lucht, *J. Electrochem. Soc.* 152 (12) (2005) A2327–A2334.
- [16] S.F. Lux, I.T. Lucas, E. Pollak, S. Passerini, M. Winter, R. Kostecki, *Electrochem. Commun.* 14 (2012) 47–50.
- [17] H. Yang, X.-D. Shen, *J. Power Sources* 167 (2007) 515–519.
- [18] M.D.S. Lekgoathi, B.M. Vilakazi, J.B. Wagener, J.P. Le Roux, D. Moolman, *J. Fluor. Chem.* 149 (2013) 53–56.
- [19] Hammami, N. Raymond, M. Armand, *Nature* 424 (2003) 635–636.
- [20] T. Ohsaki, T. Kishi, T. Kuboki, N. Takami, N. Shimura, Y. Sato, M. Sekino, A. Satoh, *J. Power Sources* 146 (2005) 97–100.
- [21] E.P. Roth, C.J. Orendorff, *Electrochem. Soc. Interface* (Summer 2012) 45–49.
- [22] D.P. Abraham, E.P. Roth, R. Kostecki, K. McCarthy, S. MacLaren, D.H. Doughty, *J. Power Sources* 161 (2006) 648–657.
- [23] M.D. Chatelain, T.E. Adams, *Proc. Power Sources Conf.* 42 (2006) 87–89.
- [24] P. Ribière, S. Grugeon, M. Morcrette, S. Boyanov, S. Laruelle, G. Marlair, *Energy Environ. Sci.* 5 (2012) 5271–5280.
- [25] G.G. Eshetu, S. Grugeon, S. Laruelle, S. Boyanov, A. Lecocq, J.-P. Bertrand, G. Marlair, *Phys. Chem. Chem. Phys.* 15 (2013) 9145–9155.
- [26] EN 13823:2010, Reaction to Fire Tests for Building Products – Building Products Excluding Floorings Exposed to the Thermal Attack by a Single Burning Item, European Committee for Standardization, Brussels, 2010.
- [27] ISO 19702:2006, Toxicity Testing of Fire Effluents – Guidance for Analysis of Gases and Vapours in Fire Effluents Using FTIR Gas Analysis, International Organization for Standardization, Geneva, 2006.
- [28] P. Andersson, P. Blomqvist, A. Lorén, F. Larsson, Investigation of Fire Emissions from Li-ion Batteries, SP Report 2013:5, SP Technical Research Institute of Sweden, Borås, Sweden, 2013, ISBN 978-91-87461-00-2.
- [29] J.M. Hollas, *Modern Spectroscopy*, third ed., John Wiley & Sons, Chichester, 1996.
- [30] C.-Y. Jhu, Y.-W. Wang, C.-M. Shu, J.-C. Chang, H.-C. Wu, *J. Hazard. Mater.* 192 (2011) 99–107.
- [31] H. Joachin, T.D. Kaun, K. Zaghib, J. Prakash, *J. Electrochem. Soc.* 156 (6) (2009) A401–A406.
- [32] G. Chen, T.J. Richardson, *J. Electrochem. Soc.* 156 (9) (2009) A756–A762.
- [33] G. Chen, T.J. Richardson, *J. Power Sources* 195 (2010) 1221–1224.
- [34] K. Zaghib, J. Dubé, A. Dallaire, K. Galoustov, A. Guerfi, M. Ramanathan, A. Benmayza, J. Prakash, A. Mauger, C.M. Julien, *J. Power Sources* 219 (2012) 36–44.
- [35] Lecocq, M. Bertana, B. Truchot, G. Marlair, in: P. Andersson, B. Sundström (Eds.), *Conference Proceedings of Fires in Vehicles (FIVE) 2012*, SP Technical Research Institute of Sweden, Borås, Sweden, 2012, pp. 183–193.